Numerical Analysis and Computational Testing of a high accuracy Leray-deconvolution model of turbulence

William Layton[1,5] Carolina C. Manica[2,5]
Monika Neda[3,5] Leo G. Rebholz[4,5]
Department of Mathematics
University of Pittsburgh PA 15260

Abstract

We study a computationally attractive algorithm (based on an extrapolated Crank-Nickolson method) for a recently proposed family of high accuracy turbulence models (the Leray-deconvolution family). First we prove convergence of the algorithm to the solution of the Navier Stokes equations (NSE) and delineate its (optimal) accuracy. Numerical experiments are presented which confirm the convergence theory. Our 3d experiments also give a careful comparison of various related approaches. They show the combination of the Leray-deconvolution regularization with the extrapolated Crank-Nicolson method can be more accurate at higher Reynolds number that the classical extrapolated trapezoidal method of Baker [6]. We also show the higher order Leray-deconvolution models (e.g. $N = 1, 2, 3$) have greater accuracy than the $N = 0$ case of the Leray-alpha model. Numerical experiments for the 2-dimensional step problem are also successfully investigated, showing the higher order models have a reduced effect on transition from one flow behavior to another. To estimate the complexity of using Leray-deconvolution models for turbulent flow simulations we estimate the models' microscale.

Key words. Leray-deconvolution model, Leray-alpha model, turbulence, deconvolution, large eddy simulation

AMS subject classifications: 65M12, 65M60, 76D05, 76F65

1 Introduction

The Leray-deconvolution (LerayDC) fluid flow model is a recently developed, high accuracy regularization of the Navier-Stokes equations (NSE). The NSE are given by

$$u_t + u \cdot \nabla u - \nu \Delta u + \nabla p = f, \quad \nabla \cdot u = 0\,, \qquad \text{in } \Omega \times (0, T). \tag{1.1}$$

In 1934, J. Leray [29, 30] introduced the following regularization of the NSE (now known as the Leray model) as a theoretical tool:

$$u_t + \overline{u} \cdot \nabla u - \nu \triangle u + \nabla p = f \text{ and } \nabla \cdot u = 0\,, \qquad \text{in } \Omega \times (0, T). \tag{1.2}$$

[1]wjl@pitt.edu, http://www.pitt.edu/∼wjl
[2]cac15@pitt.edu, http://www.pitt.edu/∼cac15
[3]mon5@pitt.edu, http://www.pitt.edu/∼mon5
[4]ler6@math.pitt.edu, http://www.math.pitt.edu/∼ler6
[5]Partially supported by NSF Grants DMS 0207627 and DMS 0508260

He chose $\overline{u} = g_\delta \star u$, where g_δ is a gaussian associated with a length scale δ and proved existence and uniqueness of strong solutions to (1.2) and convergence as $\delta \to 0$ (modulo a subsequence) to a weak solution of the NSE. If that weak solution is a smooth, strong solution it is not difficult to prove additionally that $||u_{NSE} - u_{LerayModel}|| = O(\delta^2)$ using only $||u - \overline{u}|| = O(\delta^2)$.

These and other good theoretical properties have sparked a re-examination of the Leray model (1.2) as a regularized model for simulations of turbulent flows with the modification that the gaussian filter is replaced by a less expensive differential filter, $\overline{\mathbf{u}} := (-\delta^2\triangle+1)^{-1}\mathbf{u}$. Properties of the resulting Leray-alpha model (1.2) are derived by Geurts and Holm [20, 19] test in turbulent flow simulations and the theory of the model is developed in [10, 11, 22, 39]. The form of the model, its theory and the tests of Guerts and Holm [20, 19] reveal three [1] issues:

1. $\overline{u}$ is a nonlocal function of u and so must not be treated implicitly,
2. the accuracy of the model (1.2) is strictly limited to $O(\delta^2)$, and
3. without additional terms added, simulations of the model can result in an accumulation of energy around the cutoff length scale (i.e. wiggles).

In this report we consider a related, higher order accurate family, the Leray deconvolution models [2]:

$$u_t + D_N(\overline{u}) \cdot \nabla u - \nu\triangle u + \nabla p = f \text{ and } \nabla \cdot u = 0\,, \quad \text{in } \Omega \times (0,T). \tag{1.3}$$

where D_N is a deconvolution operator, [7], satisfying for smooth u,

$$D_N\overline{u} = u + O(\delta^{2N+2}) \qquad N = 0, 1, 2, \ldots$$

The model (1.3) has the following attractive properties:

- for $N = 0$ they include the Leray/Leray-alpha model as the lowest order special case.
- their accuracy is high, $O(\delta^{2N+2})$ for arbitrary $N = 0, 1, 2, \cdots$.
- they improve upon the attractive theoretical properties of the Leray model, e.g., convergence (modulo a subsequence) as $\delta \to 0$ to a weak solution of the NSE and $||u_{NSE} - u_{LerayDCM}|| = O(\delta^{2N+2})$ for a smooth, strong solution u_{NSE}, [27].
- given $\overline{u}$ the computation of $D_N\overline{u}$ is computationally attractive.
- the higher order models (for $N \geq 1$) give dramatic improvement of accuracy and physical fidelity over the $N = 0$ case (see section 4).
- increasing model accuracy can be done in two ways: (i) cutting $\delta \to \delta/2$ increases accuracy for $N = 0$ by $\simeq 1/4$ but requires remeshing with $\simeq 8\times$ as many unknowns, and (ii) increasing $N \to N + 1$ increases accuracy from $O(\delta^{2N+2})$ to $O(\delta^{2N+4})$ and requires one more Poisson solve ($(-\delta^2\triangle + 1)^{-1}\phi$) per time step.

[1] It is also not frame invariant, Guermond, Prudhomme and Oden [18]

[2] This family of models is an idea of A. Dunca. Private communication.

- although our analysis of (1.3) is for differential filters, the model is independent of this filter choice and the analysis is extensible to many other filters with only technical modifications.

This report has two goals. First, we consider two related unconditionally stable algorithms for (1.3), the CN (Crank-Nickolson) and CNLE (Crank-Nickolson with linear extrapolation) methods, section 3. We give a numerical analysis of the CN method and tests of both CN and CNLE methods and delineate some of its *advantages* and *disadvantages* beyond the usual error analysis. The numerical analysis gives analytic insight into balancing the meshwidth h and the filtering radius δ. Second, we test the family of models themselves for accuracy and physical fidelity (section 4) and draw tentative conclusions about the Leray deconvolution family.

The ideas we test are outgrowths of the seminal work of J. Leray [29, 30], the recent work on the Leray alpha model [20, 19], the early work of G. Baker [6] on extrapolated Crank-Nicolson methods and the development of the deconvolution approach to large eddy simulation. The deconvolution approach to modelling turbulence is an ingenious idea of Stolz and Adams with Kleiser [1, 4] which has interesting and extensive mathematical justification for its accuracy and effectiveness, e.g., [2, 3, 5].

We will formally present the scheme in Section 2 after giving the notation and definitions necessary for the scheme and for the analysis used throughout this article. Section 3 develops the theory for the scheme, showing stability, existence of solutions, and analysis of convergence. Numerical experiments are presented in Section 4, followed by conclusions.

The models (1.2), (1.3) are properly regularizations of the NSE. Thus, we stress that the correct question is to study convergence of discretizations (1.2), (1.3) to solutions of the NSE as h and $\delta \to 0$ (rather than to solution of (1.2), (1.3)). This is the question we study herein.

2 Notation and Preliminaries

This section summarizes the notation, definitions and preliminary lemmas needed. We start by introducing the following notation. The $L^2(\Omega)$ norm and inner product will be denoted by $\|\cdot\|$ and $(\cdot,\cdot)$. Likewise, the $L^p(\Omega)$ norms and the Sobolev $W_p^k(\Omega)$ norms are denoted by $\|\cdot\|_{L^p}$ and $\|\cdot\|_{W_p^k}$, respectively. For the semi-norm in $W_p^k(\Omega)$ we use $|\cdot|_{W_p^k}$. H^k is used to represent the Sobolev space W_2^k, and $\|\cdot\|_k$ denotes the norm in H^k. For functions $v(x,t)$ defined on the entire time interval $(0,T)$, we define $(1 \le m < \infty)$

$$\|v\|_{\infty,k} := \operatorname*{ess\,sup}_{0<t<T} \|v(t,\cdot)\|_k\,, \qquad \text{and} \qquad \|v\|_{m,k} := \left(\int_0^T \|v(t,\cdot)\|_k^m\, dt\right)^{1/m}.$$

We consider both, the periodic case and the case of internal flow with no slip boundary conditions. (There is mainly only small notational differences between these two cases in the analysis.)

In the periodic case, $\Omega = (0,L)^d, d = 2,3$ and the velocity pressure spaces are

$$X := H^1_{\#} := \{v \in H^1(\Omega) \cap L^2_0(\Omega) :\ v \text{ is L periodic }\}\,, \qquad Q := L^2_0(\Omega)\,, \tag{2.1}$$

while in the case of internal flow Ω is a regular, bounded domain in R^d and

$$X := H^1_0(\Omega)\,, \qquad Q := L^2_0(\Omega)\,. \tag{2.2}$$

We denote the dual space of X as $X^\star$, with the norm $\|\cdot\|_\star$. The space of divergence free functions is denoted

$$V := \{v \in X, (\nabla \cdot v, q) = 0 \ \ \forall q \in Q\}. \tag{2.3}$$

The velocity-pressure finite element spaces $X^h \subset X$, $Q^h \subset Q$ are assumed to be conforming and satisfy the LBB^h condition, e.g. [17] The discretely divergence free subspace of X^h is, as usual

$$V^h = \{v^h \in X^h, (\nabla \cdot v^h, q^h) = 0 \ \ \forall q^h \in Q^h\}. \tag{2.4}$$

In addition, we make use of the following approximation properties,[9]:

$$\begin{aligned}
\inf_{v\in X_h} \|u - v\| &\leq Ch^{k+1}\|u\|_{k+1}, \ \ u \in H^{k+1}(\Omega)^d, \\
\inf_{v\in X_h} \|u - v\|_1 &\leq Ch^{k}\|u\|_{k+1}, \ \ u \in H^{k+1}(\Omega)^d, \\
\inf_{r\in Q_h} \|p - r\| &\leq Ch^{s+1}\|p\|_{s+1}, \ \ p \in H^{s+1}(\Omega).
\end{aligned} \tag{2.5}$$

Taylor-Hood elements (see e.g [9][17]) are one common example of such a choice for (X^h, Q^h), and are also the elements we use in our numerical experiments.

We employ the usual skew-symmetrization used in many finite element discretizations for fluid flow problems. Using this trilinear form ensures stability of the method.

Definition 2.1 (Skew Symmetric operator b^*). *Define the skew-symmetric trilinear form $b^* : X \times X \times X \to \mathbf{R}$ as*

$$b^*(u, v, w) := \frac{1}{2}(u \cdot \nabla v, w) - \frac{1}{2}(u \cdot \nabla w, v) \tag{2.6}$$

We now list important estimates for the b^* operator necessary in Section 3.

Lemma 2.2. *For $u, v, w \in X$, and also $v \in L_\infty(\Omega)$ for the first estimate, the trilinear term $b^*(u, v, w)$ can be bounded in the following ways*

$$b^*(u, v, w) \leq \frac{1}{2}\left(\|u\| \|\nabla v\|_\infty \|w\| + \|u\| \|v\|_\infty \|\nabla w\|\right). \tag{2.7}$$

$$b^*(u, v, w) \leq C_0(\Omega) \|\nabla u\| \|\nabla v\| \|\nabla w\| \ , \tag{2.8}$$

$$b^*(u, v, w) \leq C_0(\Omega) \|u\|^{1/2} \|\nabla u\|^{1/2} \|\nabla v\| \|\nabla w\| \ . \tag{2.9}$$

Proof. The result of the first bound follows immediately from the definition of b^*. The proof of the other two bounds can be found, for example, in [26]. □

Our analysis selects discrete differential filters. Continuous differential filters were introduced into turbulence modeling by Germano [15][16] and used in NS-α and related models [10][11][22][20],[19]. They can arise, for example, as approximations to gaussian filters of high qualitative and quantitative accuracy [14].

Definition 2.3 (Continuous differential filter). *For periodic $\phi \in L^2(\Omega)$ and $\delta > 0$ fixed, denote the filtering operation on ϕ by $\overline{\phi}$, where $\overline{\phi}$ is the unique periodic solution of*

$$-\delta^2 \Delta \overline{\phi} + \overline{\phi} = \phi. \tag{2.10}$$

We denote by $A := (-\delta^2\Delta + I)$, so $A^{-1}v = \overline{v}$. We define next the discrete differential filter following, Manica and Kaya-Merdan [32].

Definition 2.4 (Discrete differential filter). *Given $v \in L^2(\Omega)$, for a given filtering radius $\delta > 0$, $\overline{v}^h = A_h^{-1} v$ is the unique solution in X^h of*

$$\delta^2(\nabla \overline{v}^h, \nabla \chi) + (\overline{v}^h, \chi) = (v, \chi) \quad \forall \chi \in X^h. \tag{2.11}$$

Definition 2.5. *Define the L^2 projection $\Pi^h : L^2(\Omega) \to X^h$ and discrete Laplacian operator $\Delta^h : X \to X^h$ in the usual way by*

$$(\Pi^h v - v, \chi) = 0\,, \qquad (\Delta^h v, \chi) = -(\nabla v, \nabla \chi) \quad \forall \chi \in X^h. \tag{2.12}$$

With $\triangle^h$, we can write $\overline{v^h}^h = (-\delta^2 \triangle^h + \Pi^h)^{-1} v^h$ and $A_h = (-\delta^2 \triangle^h + \Pi^h)$.

Remark 2.6. *In the nonperiodic case, an important option is to define the differential filter by a discrete Stokes problem so as to preserve incompressibility approximately. In this case, given $\phi \in V$, $\overline{\phi^h}^h \in V^h$ would be defined by*

$$\delta^2(\nabla \overline{\phi^h}^h, \nabla v^h) + (\overline{\phi^h}^h, v^h) = (\phi, v^h) \text{ for all } v^h \in V^h\,.$$

This is of course a more expensive filtering operation. Herein we study the less expensive option (2.11). Discrete incompressibility is imposed on the approximate velocity directly in the model. Discrete incompressibility of $\overline{\mathbf{u}}^h$ is addressed by explicit skew-symmetrization of the trilinear form in the discrete momentum equation.

Remark 2.7 (Modification of the model). *The model (1.3) is correct as written for any filtering operation that preserves incompressibility exactly. For no-slip boundary conditions and the differential filter $\overline{u} = (-\delta^2 \triangle + 1)^{-1} u$, incompressibility is only preserved approximately (to $O(\delta^2)$). In this case the nonlinear term of the continuous model should be modified (to preserve skew-symmetry) by*

$$u_t + D_N(\overline{u}) \cdot \nabla u - \frac{1}{2}\left(\nabla \cdot D_N(\overline{u})\right) u - \nu \triangle u + \nabla p = f\ , \quad \nabla \cdot u = 0\,, \qquad \text{in } \Omega \times (0,T).$$

This modification is consistent with our use of the skew-symmetrized trilinear form in the discrete equations in all cases.

We now define the van Cittert approximate deconvolution operators.

Definition 2.8. *The continuous and discrete van Cittert deconvolution operators D_N and D_N^h are*

$$D_N v := \sum_{n=0}^{N} (I - A^{-1})^n v\,, \qquad D_N^h v := \sum_{n=0}^{N} (\Pi_h - A_h^{-1})^n v\,. \tag{2.13}$$

Our numerical experiments use $N = 0, 1, 2, 3$ for which we have for $v \in X^h$,

$$\begin{aligned} D_0^h v &= v, && (2.14)\\ D_1^h v &= 2v - \overline{v}^h, && (2.15)\\ D_2^h v &= 3v - 3\overline{v}^h + \overline{\overline{v}^h}^h, && (2.16)\\ D_3^h v &= 4v - 6\overline{v}^h + 4\overline{\overline{v}^h}^h - \overline{\overline{\overline{v}^h}^h}^h. && (2.17) \end{aligned}$$

D_N was shown to be an $O(\delta^{2N+2})$ approximate inverse to the filter operator A^{-1} in Lemma (2.1) of [12], recalled next.

Lemma 2.9. *D_N is a bounded, self-adjoint positive operator. D_N is an $O(\delta^{2N+2})$ asymptotic inverse to the filter A^{-1}. Specifically, for smooth ϕ and as $\delta \to 0$,*

$$\phi = D_N \overline{\phi} + (-1)^{(N+1)} \delta^{2N+2} \Delta^{N+1} A^{-(N+1)} \phi$$

We begin by recalling from [8], [32] some basic facts about discrete differential filters and deconvolution operators.

Lemma 2.10. *For $v \in X^h$, we have the following bounds for the discretely filtered and approximately deconvolved v*

$$\begin{aligned} \left\| \overline{v}^h \right\| &\leq \|v\| && (2.18)\\ \left\| D_N^h \overline{v}^h \right\| &\leq C(N) \|v\| && (2.19)\\ \left\| \nabla \overline{v}^h \right\| &\leq \|\nabla v\| && (2.20)\\ \left\| \nabla D_N^h \overline{v}^h \right\| &\leq C(N) \|\nabla v\| && (2.21) \end{aligned}$$

Proof. The proof of (2.18) follows from choosing $\chi = \overline{v}^h$ in (2.11), and applying Young's inequality. (2.19) follows exactly as in [8].

To prove (2.20), we note that the filter definition can be rewritten using Δ^h as

$$-\delta^2 (\Delta^h \overline{v}^h, \chi) + (\overline{v}^h, \chi) = (v, \chi) \quad \forall \chi \in X^h.$$

Choosing $\chi = \Delta^h \overline{v}^h$ and using the definition of Δ^h gives

$$\delta^2 \left\| \Delta^h \overline{v}^h \right\|^2 + \left\| \nabla \overline{v}^h \right\|^2 = (\nabla v, \nabla \overline{v})$$

Now Young's inequality proves (2.20). (2.21) follows immediately from (2.20) and the definition of D_N^h. □

Lemma 2.11. *For smooth ϕ the discrete approximate deconvolution operator satisfies*

$$\|\phi - D_N^h \overline{\phi}^h\| \leq C\delta^{2N+2} \|\overline{\phi}\|_{H^{2N+2}} + C(\delta h^k + h^{k+1}) \left(\sum_{n=1}^{N} | (A^{-1})^n \phi |_{k+1} \right). \quad (2.22)$$

Proof. We start the proof by splitting the error

$$\|\phi - D_N^h \overline{\phi}^h\| \leq \|\phi - D_N \overline{\phi}\| + \|D_N \overline{\phi} - D_N^h \overline{\phi}\| + \|D_N^h \overline{\phi} - D_N^h \overline{\phi}^h\| \,. \tag{2.23}$$

Lemma 2.9 gives

$$\|\phi - D_N \overline{\phi}\| \leq C\, \delta^{2N+2} \|\overline{\phi}\|_{H^{2N+2}} \,. \tag{2.24}$$

Lemma 2.10 gives for the third term in (2.23) that $\|D_N^h \overline{\phi} - D_N^h \overline{\phi}^h\| \leq C\|\overline{\phi} - \overline{\phi}^h\|$. Then, by using standard finite element techniques (i.e. subtracting (2.11) from the continuous scheme of (2.10) and using standard inequalities) we have

$$\|\overline{\phi} - \overline{\phi}^h\| \leq C(\delta h^k + h^{k+1}) |\overline{\phi}|_{k+1} \,. \tag{2.25}$$

It is left to bound the second term from (2.23). First, note that for $N = 0$, $\|D_0 \overline{\phi}^h - D_0^h \overline{\phi}^h\| = 0$. Based on the Definition 2.8 of continuous and discrete deconvolution operators and their expansion (see (2.14)- (2.17)), we note that D_N is a polynomial of degree N in A^{-1} (and D_N^h in A_h^{-1} as well). Thus, the second term in (2.23) can be written as

$$\|D_N \overline{\phi} - D_N^h \overline{\phi}\| = \| \sum_{n=0}^{N} \alpha_n \left((A^{-1})^n \overline{\phi} - (A_h^{-1})^n \overline{\phi} \right) \| \leq \sum_{n=0}^{N} \alpha_n \|(A^{-1})^n \overline{\phi} - (A_h^{-1})^n \overline{\phi}\| \,. \tag{2.26}$$

For $O(1)$ coefficients α_n and for $N = 1$, the results (2.25) and (2.18) give

$$\begin{aligned} \|(A^{-1})\overline{\phi} - (A_h^{-1})\overline{\phi}\| &= \|\overline{\overline{\phi}} - \overline{\overline{\phi}^h}\| \\ &\leq \|\overline{\overline{\phi}} - \overline{\overline{\phi}}^h\| + \|\overline{\overline{\phi}}^h - \overline{\overline{\phi}^h}\| \\ &\leq \|\overline{\overline{\phi}} - \overline{\overline{\phi}}^h\| + \|\overline{\phi} - \overline{\phi}^h\| \\ &\leq C(\delta h^k + h^{k+1}) \left(|\overline{\overline{\phi}}|_{k+1} + |\overline{\phi}|_{k+1} \right) . \end{aligned} \tag{2.27}$$

Inductively,

$$\|(A^{-1})^N \overline{\phi} - (A_h^{-1})^N \overline{\phi}\| \leq C(\delta h^k + h^{k+1}) (\sum_{n=1}^{N} | \, (A^{-1})^n \phi \, |_{k+1} \,) \,. \tag{2.28}$$

The proof is completed by combining the derived bounds for the terms in (2.23). □

Recall that a strong solution of the Navier Stokes equations satisfies $u \in L^2(0,T;X) \cap L^\infty(0,T;L^2(\Omega)) \cap L^4(0,T;X)$, $p \in L^2(0,T;Q)$ with $\mathbf{u}_t \in L^2(0,T;X')$ such that

$$(u_t, v) + (u \cdot \nabla u, v) - (p, \nabla \cdot v) + \nu(\nabla u, \nabla v) = (f, v) \;,\; \forall v \in X \,, \tag{2.29}$$

$$(q, \nabla \cdot u) = 0 \;,\; \forall q \in Q \,. \tag{2.30}$$

For simplicity and clarity of notation we let $v(t_{n+1/2}) = v((t_n + t_{n+1})/2)$ for the continuous variable and $v_{n+1/2} = (v_n + v_{n+1})/2$ for both, continuous and discrete variables.

Algorithm 2.12. *[Crank-Nicholson Finite Element Scheme for Leray-deconvolution] Let* $\Delta t > 0$, $(w_0, q_0) \in (X^h, Q^h)$, $f \in X^*$ *and* $M := \frac{T}{\Delta t}$ *For* $n = 0, 1, 2, \cdots, M-1$, *find* $(w^h_{n+1}, q^h_{n+1}) \in (X^h, Q^h)$ *satisfying*

$$\frac{1}{\Delta t}(w^h_{n+1} - w^h_n, v^h) + b^*(D^h_N \overline{w^h_{n+1/2}}^h, w^h_{n+1/2}, v^h) - (q^h_{n+1/2}, \nabla \cdot v^h) + \nu(\nabla w^h_{n+1/2}, \nabla v^h) = (f_{n+1/2}, v^h) \ \forall \ v^h \in X^h \quad (2.31)$$

$$(\nabla \cdot w^h_{n+1}, \chi^h) = 0 \ \forall \chi^h \in Q^h \quad (2.32)$$

Remark 1. *Since* (X^h, Q^h) *satisfies the LBB*^{h} *condition, (2.31)-(2.32) is equivalent to*

$$\frac{1}{\Delta t}(w^h_{n+1} - w^h_n, v^h) + b^*(D^h_N \overline{w^h_{n+1/2}}^h, w^h_{n+1/2}, v^h) + \nu(\nabla w^h_{n+1/2}, \nabla v^h) = (f_{n+1/2}, v^h) \ \forall \ v^h \in V^h. \quad (2.33)$$

Note that for the CNLE implementation of Algorithm 4.1, it is the deconvolved term that is extrapolated. In CNLE, this term is from (known) previous time levels and so the deconvolution is treated explicitly. This is particularly effective for (1.2) and (1.3). We have also tested quadratic extrapolation. The preliminary results are much better qualitatively than linear extrapolation.

Lemma 2.13.

$$\left\|u_{n+1/2} - u(t_{n+1/2})\right\|^2 \ \leq \ \frac{1}{48}(\Delta t)^3 \int_{t_n}^{t_{n+1}} \|u_{tt}\|^2 \ dt\,, \quad (2.34)$$

$$\left\|\frac{u_{n+1} - u_n}{\Delta t} - u_t(t_{n+1/2})\right\|^2 \ \leq \ \frac{1}{1280}(\Delta t)^3 \int_{t_n}^{t_{n+1}} \|u_{ttt}\|^2 \ dt\,, \ \textit{and} \quad (2.35)$$

$$\left\|\nabla(u_{n+1/2} - u(t_{n+1/2})\right\|^2 \ \leq \ \frac{(\Delta t)^3}{48} \int_{t_n}^{t_{n+1}} \|\nabla u_{tt}\|^2 \ dt\,. \quad (2.36)$$

The proof of Lemma 2.13 is based on the Taylor expansion with remainder. It is more of technical nature and therefore omitted herein.

The error analysis uses a discrete Gronwall inequality, recalled from [25], for example.

Lemma 2.14 (Discrete Gronwall Lemma). *Let* Δt, H, *and* a_n, b_n, c_n, d_n *(for integers* $n \geq 0$*) be nonnegative numbers such that*

$$a_l + \Delta t \sum_{n=0}^{l} b_n \leq \Delta t \sum_{n=0}^{l} d_n a_n + \Delta t \sum_{n=0}^{l} c_n + H \quad \textit{for } l \geq 0. \quad (2.37)$$

Suppose that $\Delta t d_n < 1 \ \forall n$. *Then,*

$$a_l + \Delta t \sum_{n=0}^{l} b_n \leq exp\left(\Delta t \sum_{n=0}^{l} \frac{d_n}{1 - \Delta t d_n}\right)\left(\Delta t \sum_{n=0}^{l} c_n + H\right) \quad \textit{for } l \geq 0. \quad (2.38)$$

In the discrete case we use the analogous norms:

$$|||v|||_{\infty,k} := \max_{0 \leq n \leq N_T} \|v^n\|_k\,, \qquad |||v_{1/2}|||_{\infty,k} := \max_{1 \leq n \leq N_T} \|v^{n-1/2}\|_k\,,$$

$$|||v|||_{m,k} := \left(\sum_{n=0}^{N_T} \|v^n\|_k^m \triangle t\right)^{1/m}, \qquad |||v_{1/2}|||_{m,k} := \left(\sum_{n=1}^{N_T} \|v^{n-1/2}\|_k^m \triangle t\right)^{1/m}.$$

3 Analysis of full Crank-Nickolson Scheme

In this section, we show that solutions of the scheme (2.33), equivalently (2.31)-(2.32) are unconditionally stable, well defined and optimally convergent to solutions of the NSE. This error analysis, already technical, can be extended to the CNLE time stepping method.

Lemma 3.1. *Consider the approximation scheme (4.1). A solution u_h^l, $l = 1, \dots M$, exists at each timestep. The scheme is also unconditionally stable. It satisfies the following á priori bound:*

$$\left\|w_M^h\right\|^2 + \nu\Delta t \sum_{n=0}^{M-1} \left\|\nabla w_{n+1/2}^h\right\|^2 \leq \left\|w_0^h\right\|^2 + \frac{\Delta t}{\nu} \sum_{n=0}^{M-1} \left\|f_{n+1/2}\right\|_*^2 . \tag{3.1}$$

Proof. : The existence of a solution u_h^n to (4.1) follows from the Leray-Schauder Principle [40]. Specifically, let $A : V^h \to V^h$, be defined by $y = A(z)$ satisfying

$$\begin{aligned}(y, v) := -\triangle t b^*(D_N^h \overline{(z + w_n^h)/2}^h, (z + w_n^h)/2, v) - \triangle t\nu(\nabla(z + w_n^h)/2, \nabla v) \\ +(w_{n-1}^h, v) + \triangle t(f_{n+1/2}, v) .\end{aligned}$$

The operator A is compact and any solution of $u = s\,A(u)$, for $0 \leq s < 1$, satisfies the bound $\|u\| \leq \gamma$, where γ is independent of s. Thus, a solution exists.

To obtain the á priori estimate set $v^h = w_{n+1/2}^h$ in (2.33)

$$\frac{1}{2\Delta t}(\left\|w_{n+1}^h\right\|^2 - \left\|w_n^h\right\|^2) + \nu \left\|\nabla w_{n+1/2}^h\right\|^2 \leq \frac{1}{2\nu} \left\|f_{n+1/2}\right\|_*^2 + \frac{\nu}{2} \left\|\nabla w_{n+1/2}^h\right\|^2 \quad \text{for every } n,$$

i.e.,

$$\frac{1}{\Delta t}(\left\|w_{n+1}^h\right\|^2 - \left\|w_n^h\right\|^2) + \nu \left\|\nabla w_{n+1/2}^h\right\|^2 \leq \frac{1}{\nu} \left\|f_{n+1/2}\right\|_*^2, \quad \text{for every } n.$$

Summing from $n = 0 \dots M - 1$ gives the desired result. □

Our main convergence estimates are given next.

Theorem 3.2. *Let $(u(t), p(t))$ be a sufficiently smooth, strong solution of the NSE (1.1) satisfying either no-slip or periodic with zero-mean boundary conditions. Suppose (w_0^h, q_0^h) are approximations of $(u(0), p(0))$ to the accuracy of (2.5), respectively. Then there is a constant $C = C(u, p)$ such that*

$$|||u - w^h|||_{\infty,0} \leq F(\triangle t, h, \delta) + Ch^{k+1}|||u|||_{\infty,k+1} , \tag{3.2}$$

$$\begin{aligned}\left(\nu\triangle t \sum_{n=0}^{M-1} \|\nabla(u^{n+1/2} - (w_{n+1}^h + w_n^h)/2)\|^2\right)^{1/2} &\leq F(\triangle t, h, \delta) + C\nu^{1/2}(\triangle t)^2\|\nabla u_{tt}\|_{2,0} \\ &\quad + C\nu^{1/2}h^k|||u|||_{2,k+1} .\end{aligned} \tag{3.3}$$

where

$$
\begin{aligned}
F(\triangle t,h,\delta) &:= C\nu^{-1/2}\,h^{k+1/2}\left(|||u|||^2_{4,k+1}+|||\nabla u|||^2_{4,0}\right)+C\nu^{1/2}h^k|||u|||_{2,k+1}\\
&+C\nu^{-1/2}h^k\left(|||u|||^2_{4,k+1}+\nu^{-1/2}(\|w_0^h\|+\nu^{-1/2}|||f|||_{2,\star})\right)+C\nu^{-1/2}h^{s+1}|||p_{1/2}|||_{2,s+1}\\
&+C\nu^{-1/2}\delta^{2N+2}\|\overline{u}\|_{2,2N+2}+C\nu^{-1/2}(\delta h^k+h^{k+1})(\sum_{n=1}^{N}\|\ (A^{-1})^n u\ \|_{2,k+1}\,)\\
&+C(\Delta t)^2\left(\|u_{ttt}\|_{2,0}+\nu^{-1/2}\|p_{tt}\|_{2,0}+\|f_{tt}\|_{2,0}\right.\\
&\qquad+\nu^{1/2}\|\nabla u_{tt}\|_{2,0}\ +\nu^{-1/2}\|\nabla u_{tt}\|^2_{4,0}\\
&\qquad\left.+\nu^{-1/2}|||\nabla u|||^2_{4,0}\ +\nu^{-1/2}|||\nabla u_{1/2}|||^2_{4,0}\right)\ .
\end{aligned}
\tag{3.4}
$$

Corollary 3.3. *Suppose that in addition to the assumptions made in Theorem 3.2, the finite element spaces X^h and Q^h are composed of Taylor-Hood elements. Then the error in the extrapolated trapezoidal finite element scheme for Leray-deconvolution is of the order*

$$
|||u-w^h|||_{\infty,0}+\left(\nu\Delta t\sum_{n=1}^{M}\|\nabla(u_{n+1/2}-w^h_{n+1/2})\|^2\right)^{1/2}=O(h^2+\Delta t^2+\delta^{2N+2}).
\tag{3.5}
$$

Proof of Theorem 3.2. Note that for $v,\ w,\ \in X$, with $u\in V$,

$$
b^*(u,v,w)\ =b(u,v,w)\ :=\ (u\cdot\nabla v,w)\ .
$$

Then, at time $t_{n+1/2}$, u given by (2.29)-(2.30) satisfies

$$
\begin{aligned}
(\frac{u_{n+1}-u_n}{\Delta t},v^h)+b^*(D_N^h\overline{u_{n+1/2}}^h,u_{n+1/2},v^h)+\nu(\nabla u_{n+1/2},\nabla v^h)-(p_{n+1/2},\nabla\cdot v^h)\\
=(f_{n+1/2},v^h)+Intp(u^n,p^n;v^h),
\end{aligned}
\tag{3.6}
$$

for all $v^h\in V^h$, where $Intp(u_n,p_n;v^h)$, representing the interpolating error, denotes

$$
\begin{aligned}
Intp(u^n,p^n;v^h)\ \ =\ \ &\left(\frac{u^{n+1}-u^n}{\Delta t}-u_t(t_{n+1/2}),v^h\right)+\nu(\nabla u_{n+1/2}\ -\ \nabla u(t_{n+1/2}),\nabla v^h)\\
&+b^*(u_{n+1/2},u_{n+1/2},v^h)-b^*(u(t_{n+1/2}),u(t_{n+1/2}),v^h)\\
&-b^*(u_{n+1/2}-D_N^h\overline{u_{n+1/2}}^h,u_{n+1/2},v^h)\\
&-(p_{n+1/2}-p(t_{n+1/2}),\nabla\cdot v^h)+(f(t_{n+1/2})-f_{n+1/2},v^h)\,.
\end{aligned}
\tag{3.7}
$$

Subtracting (3.6) from (2.33) and letting $e_n=u_n-w_n^h$ we have

$$
\begin{aligned}
\frac{1}{\Delta t}(e_{n+1}-e_n,v^h)+b^*(D_N^h\overline{u_{n+1}}^h,u_{n+1/2},v^h)-b^*(D_N^h\overline{w^h_{n+1/2}}^h,w^h_{n+1/2},v^h)+\\
\nu(\nabla e_{n+1/2},\nabla v^h)=(p_{n+1/2},\nabla\cdot v^h)+Intp(u^n,p^n;v^h)\quad\forall v^h\in V^h.
\end{aligned}
\tag{3.8}
$$

Decompose the error as $e_n=(u_n-U_n)-(w_n^h-U_n):=\eta_n-\phi_n^h$ where $\phi_n^h\in V^h$. Setting $v^h=\phi^h_{n+1/2}$ in (3.8) and using $(q,\nabla\cdot\phi_{n+1/2})=0$ for all $q\in V^h$ we obtain

$$
\begin{aligned}
(\phi^h_{n+1}-\phi^h_n,\phi^h_{n+1/2})+\nu\triangle t\|\nabla\phi^h_{n+1/2}\|+\triangle t\,b^*(D_N^h\overline{w^h_{n+1}}^h,e_{n+1/2},\phi^h_{n+1/2})\\
+\triangle t\,b^*(D_N^h\overline{e_{n+1/2}}^h,u_{n+1/2},\phi^h_{n+1/2})=(\eta_{n+1}-\eta_n,\phi^h_{n+1/2})+\triangle t\nu(\nabla\eta_{n+1/2},\nabla\phi^h_{n+1/2})\\
+\triangle t(p_{n+1/2}-q,\nabla\cdot\phi^h_{n+1/2})+\triangle t\,Intp(u^n,p^n;v^h)\,.
\end{aligned}
\tag{3.9}
$$

i.e.,

$$\frac{1}{2}(\|\phi^h_{n+1}\| - \|\phi^h_n\|) + \nu\triangle t\|\nabla\phi^h_{n+1/2}\| = (\eta_{n+1}-\eta_n, \phi^h_{n+1/2}) + \triangle t\nu(\nabla\eta_{n+1/2}, \nabla\phi^h_{n+1/2})$$
$$- \triangle t\, b^*(D^h_N\overline{\eta_{n+1/2}}^h, u_{n+1/2}, \phi^h_{n+1/2}) + \triangle t\, b^*(D^h_N\overline{\phi^h_{n+1/2}}^h, u_{n+1/2}, \phi^h_{n+1/2})$$
$$- \triangle t\, b^*(D^h_N\overline{w^h_{n+1/2}}^h, \eta_{n+1/2}, \phi^h_{n+1/2}) + \triangle t(p_{n+1/2}-q, \nabla\cdot\phi^h_{n+1/2})$$
$$+ \triangle t\, Intp(u^n, p^n; v^h)\,. \tag{3.10}$$

We now bound the terms in the RHS of (3.9) individually.
$(\eta_{n+1}-\eta_n, \phi^h_{n+1/2}) = 0$ since U is the L^2 projection of u in V^h.
Cauchy-Schwarz and Young's inequalities give

$$\begin{aligned}\nu\triangle t(\nabla\eta_{n+1/2}, \nabla\phi^h_{n+1/2}) &\le \nu\triangle t\|\nabla\eta_{n+1/2}\|\,\|\nabla\phi^h_{n+1/2}\| \\ &\le \frac{\nu\Delta t}{12}\left\|\nabla\phi^h_{n+1/2}\right\|^2 + C\nu\Delta t\left\|\nabla\eta_{n+1/2}\right\|^2. \end{aligned}\tag{3.11}$$

$$\begin{aligned}\triangle t(p_{n+1/2}-q, \nabla\cdot\phi^h_{n+1/2}) &\le C\triangle t\|p_{n+1/2}-q\|\,\|\nabla\phi^h_{n+1/2}\| \\ &\le \frac{\nu\Delta t}{12}\left\|\nabla\phi^h_{n+1/2}\right\|^2 + C\triangle t\nu^{-1}\|p_{n+1/2}-\chi^h\|^2. \end{aligned}\tag{3.12}$$

Lemmas 2.2, 2.10 and standard inequalities give

$$\begin{aligned}&\triangle t\, b^*(D^h_N\overline{\eta_{n+1/2}}^h, u_{n+1/2}, \phi^h_{n+1/2}) \\ \le\ & C\Delta t\|D^h_N\overline{\eta_{n+1/2}}^h\|^{1/2}\,\|\nabla D^h_N\overline{\eta_{n+1/2}}^h\|^{1/2}\,\|\nabla u_{n+1/2}\|\,\|\nabla\phi^h_{n+1/2}\| \\ \le\ & \frac{\nu\triangle t}{12}\|\phi^h_{n+1/2}\|^2 + C\triangle t\,\nu^{-1}\|\eta_{n+1/2}\|\,\|\nabla\eta_{n+1/2}\|\|\nabla u_{n+1/2}\|^2. \end{aligned}\tag{3.13}$$

$$\begin{aligned}&\triangle t\, b^*(D^h_N\overline{\phi^h_{n+1/2}}^h, u_{n+1/2}, \phi^h_{n+1/2}) \\ \le\ & C\triangle t\|D^h_N\overline{\phi^h_{n+1/2}}^h\|^{1/2}\,\|\nabla D^h_N\overline{\phi^h_{n+1/2}}^h\|^{1/2}\,\|\nabla u_{n+1/2}\|\,\|\nabla\phi^h_{n+1/2}\| \\ \le\ & C\triangle t\|\phi^h_{n+1/2}\|^{1/2}\,\|\nabla\phi^h_{n+1/2}\|^{3/2}\,\|\nabla u_{n+1/2}\| \\ \le\ & \frac{\nu\triangle t}{12}\|\nabla\phi^h_{n+1/2}\|^{1/2} + C\triangle t\,\nu^{-3}\|\phi^h_{n+1/2}\|^2\,\|\nabla u_{n+1/2}\|^4. \end{aligned}\tag{3.14}$$

$$\begin{aligned}&\triangle t\, b^*(D^h_N\overline{w^h_{n+1/2}}^h, \eta_{n+1/2}, \phi^h_{n+1/2}) \\ \le\ & C\|D^h_N\overline{w^h_{n+1/2}}^h\|^{1/2}\,\|\nabla D^h_N\overline{w^h_{n+1/2}}^h\|^{1/2}\,\|\nabla\eta_{n+1/2}\|\,\|\nabla\phi^h_{n+1/2}\| \\ \le\ & \frac{\nu\triangle t}{12}\|\nabla\phi^h_{n+1/2}\|^2 + C\triangle t\,\nu^{-1}\|w^h_{n+1/2}\|\,\|\nabla w^h_{n+1/2}\|\,\|\nabla\eta_{n+1/2}\|^2. \end{aligned}\tag{3.15}$$

Combining (3.12), (3.11), (3.13), (3.14), (3.15) and summing from $n = 0$ to $M-1$ (assuming that $\|\phi_0^h\| = 0$) reduces (3.10) to

$$\begin{aligned}
&\|\phi_M^h\|^2 + \nu\triangle t \sum_{n=0}^{M-1} \|\nabla\phi_{n+1/2}^h\|^2 \\
\leq\ & \triangle t \sum_{n=0}^{M-1} C\nu^{-3}\|\nabla u_{n+1/2}\|^4 \|\phi_{n+1/2}^h\|^2 + \triangle t \sum_{n=0}^{M-1} C\nu\|\nabla\eta_{n+1/2}\|^2 \\
&+\triangle t \sum_{n=0}^{M-1} C\nu^{-1}\|\eta_{n+1/2}\| \|\nabla\eta_{n+1/2}\|\|\nabla u_{n+1/2}\|^2 \\
&+\triangle t \sum_{n=0}^{M-1} C\nu^{-1}\|w_{n+1/2}^h\| \|\nabla w_{n+1/2}^h\| \|\nabla\eta_{n+1/2}\|^2 \\
&+\triangle t \sum_{n=0}^{M-1} C\nu^{-1}\|p_{n+1/2} - q\|^2 + \triangle t \sum_{n=0}^{M-1} C|Intp(u_n, p_n\phi_{n+1/2}^h)|\,. \qquad (3.16)
\end{aligned}$$

Now, we continue to bound the terms on the RHS of (3.16). We have that

$$\begin{aligned}
\triangle t \sum_{n=0}^{M-1} C\nu\|\nabla\eta_{n+1/2}\|^2 &\leq \triangle t C\nu \sum_{n=0}^{M} \|\nabla\eta_n\|^2 \leq \triangle t C\nu \sum_{n=0}^{M} h^{2k}|u^n|_{k+1}^2 \\
&\leq C\nu h^{2k}\||u|\|_{2,k+1}^2\,. \qquad (3.17)
\end{aligned}$$

For the term

$$\begin{aligned}
&\triangle t \sum_{n=0}^{M-1} C\nu^{-1}\|\eta_{n+1/2}\| \|\nabla\eta_{n+1/2}\| \|\nabla u_{n+1/2}\|^2 \\
\leq\ & C\nu^{-1}\triangle t \sum_{n=0}^{M-1} (\|\eta_{n+1}\| \|\nabla\eta_{n+1}\| + \|\eta_n\| \|\nabla\eta_n\| \\
&\qquad + \|\eta_n\| \|\nabla\eta_{n+1}\| + \|\eta_{n+1}\| \|\nabla\eta_n\|) \|\nabla u_{n+1/2}\|^2 \\
\leq\ & C\,\nu^{-1}\,h^{2k+1}\left(\triangle t \sum_{n=0}^{M-1} |u_{n+1}|_{k+1}^2 \|\nabla u_{n+1/2}\|^2 + \triangle t \sum_{n=0}^{M-1} |u_{n+1}|_{k+1}|u_n|_{k+1} \|\nabla u_{n+1/2}\|^2\right. \\
&\qquad \left. +\ \triangle t \sum_{n=0}^{M-1} |u_n|_{k+1}^2 \|\nabla u_{n+1/2}\|^2\right) \\
\leq\ & C\nu^{-1}\,h^{2k+1}\left(\triangle t \sum_{n=0}^{M} |u_n|_{k+1}^4 + \triangle t \sum_{n=0}^{l} \|\nabla u_n\|^4\right) \\
=\ & C\nu^{-1}\,h^{2k+1}\left(\||u|\|_{4,k+1}^4 + \||\nabla u|\|_{4,0}^4\right)\,. \qquad (3.18)
\end{aligned}$$

Using the a priori estimate for $\|w_n^h\|$, (3.1),

$$\begin{aligned}
&\triangle t \sum_{n=0}^{M-1} C\nu^{-1} \left(\|w_{n+1/2}^h\| \, \|\nabla w_{n+1/2}^h\| \, \|\nabla \eta_{n+1/2}\|^2 \right) \\
\leq \;& C\nu^{-1} \triangle t \sum_{n=0}^{M-1} \|\nabla w_{n+1/2}^h\| \, \|\nabla \eta_{n+1/2}\|^2 \\
\leq \;& C\nu^{-1} \triangle t \sum_{n=0}^{M-1} \left(\|\nabla \eta_{n+1}\|^2 + \|\nabla \eta_n\|^2 \right) \|\nabla w_{n+1/2}^h\| \\
\leq \;& C\nu^{-1} h^{2k} \triangle t \sum_{n=0}^{M-1} \left(|u_{n+1}|_{k+1}^2 + |u_n|_{k+1}^2 \right) \|\nabla u_{n+1/2}^h\| \\
\leq \;& C\nu^{-1} h^{2k} \left(\triangle t \sum_{n=0}^{M} |u^n|_{k+1}^4 + \triangle t \sum_{n=0}^{M} \|\nabla u_{n+1/2}^h\|^2 \right) \\
\leq \;& C\nu^{-1} h^{2k} \left(|||u|||_{4,k+1}^4 + \nu^{-1} (\|w_0^h\|^2 + \nu^{-1} |||f|||_{2,\star}^2) \right) . \qquad (3.19)
\end{aligned}$$

From (2.13),

$$\begin{aligned}
&\triangle t \sum_{n=0}^{M-1} C\nu^{-1} \|p_{n+1/2} - q\|^2 \leq C\nu^{-1} \triangle t \sum_{n=0}^{M-1} \|p(t_{n+1/2}) - q\|^2 + \|p_{n+1/2} - p(t_{n+1/2})\|^2 \\
\leq \;& C\nu^{-1} \left(h^{2s+2} \triangle t \sum_{n=0}^{M-1} \|p(t_{n+1/2})\|_{s+1}^2 + \triangle t \sum_{n=0}^{M-1} \frac{1}{48} (\triangle t)^3 \int_{t_n}^{t_{n+1}} \|p_{tt}\|^2 \, dt \right) \\
\leq \;& C\nu^{-1} \left(h^{2s+2} |||p_{1/2}|||_{2,s+1}^2 + (\triangle t)^4 \|p_{tt}\|_{2,0}^2 \right) \qquad (3.20)
\end{aligned}$$

We now bound the terms in $Intp(u_n, p_n; \phi_{n+1/2}^h)$. Using Cauchy-Schwarz and Young's inequalities, Taylor's theorem, and Lemma 2.11,

$$\begin{aligned}
&\left(\frac{u^{n+1} - u_n}{\Delta t} - u_t(t_{n+1/2}), \phi_{n+1/2}^h \right) \\
\leq \;& \frac{1}{2} \|\phi_{n+1/2}^h\|^2 + \frac{1}{2} \| \frac{u^{n+1} - u_n}{\Delta t} - u_t(t_{n+1/2}) \|^2 \\
\leq \;& \frac{1}{2} \|\phi_{n+1}^h\|^2 + \frac{1}{2} \|\phi_n^h\|^2 + \frac{1}{2} \frac{(\Delta t)^3}{1280} \int_{t_n}^{t_{n+1}} \|u_{ttt}\|^2 \, dt \, , \qquad (3.21)
\end{aligned}$$

$$\begin{aligned}
&(p_{n+1/2} - p(t_{n+1/2}), \nabla \cdot \phi_{n+1/2}^h) \\
\leq \;& \varepsilon_1 \nu \|\nabla \phi_{n+1/2}^h\|^2 + C \, \nu^{-1} \|p_{n+1/2} - p(t_{n+1/2})\|^2 \\
\leq \;& \varepsilon_1 \nu \|\nabla \phi_{n+1/2}^h\|^2 + C \, \nu^{-1} \frac{(\Delta t)^3}{48} \int_{t_n}^{t_{n+1}} \|p_{tt}\|^2 \, dt \, , \qquad (3.22)
\end{aligned}$$

$$\begin{aligned}
&(f(t_{n+1/2}) - f_{n+1/2}, \phi_{n+1/2}^h) \\
\leq \;& \frac{1}{2} \|\phi_{n+1/2}^h\|^2 + \frac{1}{2} \|f(t_{n+1/2}) - f_{n+1/2}\|^2 \\
\leq \;& \frac{1}{2} \|\phi_{n+1}^h\|^2 + \frac{1}{2} \|\phi_n^h\|^2 + \frac{(\Delta t)^3}{48} \int_{t_n}^{t_{n+1}} \|f_{tt}\|^2 \, dt \, , \qquad (3.23)
\end{aligned}$$

$$
\begin{aligned}
&(\nabla u_{n+1/2} - \nabla u(t_{n+1/2}), \nabla \phi^h_{n+1/2}) \\
\leq\ & \varepsilon_2 \nu \, \|\nabla \phi^h_{n+1/2}\|^2 + C\,\nu \|\nabla u_{n+1/2} - \nabla u(t_{n+1/2})\|^2 \\
\leq\ & \varepsilon_2 \nu \, \|\nabla \phi^h_{n+1/2}\|^2 + C\,\nu \frac{(\Delta t)^3}{48} \int_{t_n}^{t_{n+1/2}} \|\nabla u_{tt}\|^2 \, dt \,, \qquad (3.24)
\end{aligned}
$$

$$
\begin{aligned}
& b^*(u_{n+1/2}, u_{n+1/2}, \phi^h_{n+1/2}) - b^*(u(t_{n+1/2}), u(t_{n+1/2}), \phi^h_{n+1/2}) \\
=\ & b^*(u_{n+1/2} - u(t_{n+1/2}), u_{n+1/2}, \phi^h_{n+1/2}) - b^*(u(t_{n+1/2}), u_{n+1/2} - u(t_{n+1/2}), \phi^h_{n+1/2}) \\
\leq\ & C \, \|\nabla(u_{n+1/2} - u(t_{n+1/2}))\| \, \|\nabla \phi^h_{n+1/2}\| \, \left(\|\nabla u_{n+1/2}\| + \|\nabla u(t_{n+1/2})\| \right) \\
\leq\ & C\,\nu^{-1} \left(\|\nabla u_{n+1/2}\|^2 + \|\nabla u(t_{n+1/2})\|^2 \right) \frac{(\Delta t)^3}{48} \int_{t_n}^{t_{n+1}} \|\nabla u_{tt}\|^2 \, dt + \varepsilon_3 \nu \|\nabla \phi^h_{n+1/2}\|^2 \\
\leq\ & C\,\nu^{-1} \frac{(\Delta t)^3}{48} \left(\int_{t_n}^{t_{n+1}} 2(\|\nabla u_{n+1/2}\|^4 + \|\nabla u(t_{n+1/2})\|^4) \, dt \right. \\
& \left. + \int_{t_n}^{t_{n+1}} \|\nabla u_{tt}\|^4 \, dt \right) + \varepsilon_3 \nu \|\nabla \phi^h_{n+1/2}\|^2 \\
\leq\ & C\,\nu^{-1} \, (\Delta t)^4 (\|\nabla u_{n+1/2}\|^4 + \|\nabla u(t_{n+1/2})\|^4) \\
& + C\,\nu^{-1} \, (\Delta t)^3 \int_{t_n}^{t_{n+1}} \|\nabla u_{tt}\|^4 \, dt + \varepsilon_3 \nu \|\nabla \phi^h_{n+1/2}\|^2 \,. \qquad (3.25)
\end{aligned}
$$

$$
\begin{aligned}
& b^*(u_{n+1/2} - D^h_N \overline{u_{n+1/2}}^h, u_{n+1/2}, \phi^h_{n+1/2}) \\
\leq\ & \frac{1}{2} \Big(\|u_{n+1/2} - D^h_N \overline{u_{n+1/2}}^h\| \, \|\nabla u_{n+1/2}\|_\infty \, \|\phi^h_{n+1/2}\| \\
& + \|u_{n+1/2} - D^h_N \overline{u_{n+1/2}}^h\| \, \|u_{n+1/2}\|_\infty \, \|\nabla \phi^h_{n+1/2}\| \Big) \\
\leq\ & C \, \|u_{n+1/2} - D^h_N \overline{u_{n+1/2}}^h\| \, \|\nabla \phi^h_{n+1/2}\| \\
\leq\ & \varepsilon_4 \nu \|\nabla \phi^h_{n+1/2}\| + C \nu^{-1} \|u_{n+1/2} - D^h_N \overline{u_{n+1/2}}^h\|^2 \\
\leq\ & \varepsilon_4 \nu \|\nabla \phi^h_{n+1/2}\| + \ C \nu^{-1} \delta^{4N+4} \|\overline{u}\|^2_{H^{2N+2}} \\
& + C \nu^{-1} (\delta^2 h^{2k} + h^{2k+2}) \Big(\sum_{n=1}^{N} | \ (A^{-1})^N u \ |^2_{k+1} \Big) \,. \qquad (3.26)
\end{aligned}
$$

Combine (3.21)-(3.26) to obtain

$$
\begin{aligned}
\Delta t \sum_{n=0}^{M-1} |Intp(u^n, p^n; \phi^h_{n+1/2})| \ \leq\ & \Delta t \, C \|\phi^h_{n+1}\|^2 + (\varepsilon_1 + \varepsilon_2 + \varepsilon_3 + \varepsilon_4) \Delta t \, \nu \|\nabla \phi^h_{n+1/2}\|^2 \\
& + C \nu^{-1} \delta^{4N+4} \|\overline{u}\|^2_{2,2N+2} \\
& + C \nu^{-1} (\delta^2 h^{2k} + h^{2k+2}) \Big(\sum_{n=1}^{N} \| \ (A^{-1})^N u \ \|^2_{2,k+1} \Big) \\
& + C (\Delta t)^4 \left(\|u_{ttt}\|^2_{2,0} + \nu^{-1} \|p_{tt}\|^2_{2,0} + \|f_{tt}\|^2_{2,0} \right. \\
& \qquad + \nu \|\nabla u_{tt}\|^2_{2,0} + \nu^{-1} \|\nabla u_{tt}\|^4_{4,0} \\
& \qquad \left. + \nu^{-1} \| |\nabla u| \|^4_{4,0} + \nu^{-1} \| |\nabla u_{1/2}| \|^4_{4,0} \right) \,. \qquad (3.27)
\end{aligned}
$$

Let $\varepsilon_1 = \varepsilon_2 = \varepsilon_3 = \varepsilon_4 = 1/12$ and with (3.17)-(3.20), (3.27), from (3.16) we obtain

$$
\begin{aligned}
&\|\phi_M^h\|^2 + \nu\triangle t \sum_{n=0}^{M-1} \|\nabla\phi_{n+1/2}^h\|^2 \\
\leq\ & \triangle t \sum_{n=0}^{M-1} C(\nu^{-3}\|\nabla u_{n+1/2}\|^4 + 1)\,\|\phi_{n+1/2}^h\|^2 + C\nu h^{2k}|||u|||_{2,k+1}^2 \\
&+C\nu^{-1}\,h^{2k+1}\left(|||u|||_{4,k+1}^4 + |||\nabla u|||_{4,0}^4\right) \\
&+C\nu^{-1}h^{2k}\left(|||u|||_{4,k+1}^4 + \nu^{-1}(\|w_0^h\|^2 + \nu^{-1}|||f|||_{2,\star}^2)\right) + C\nu^{-1}h^{2s+2}|||p_{1/2}|||_{2,s+1}^2 \\
&+C\nu^{-1}\delta^{4N+4}\|\overline{u}\|_{2,2N+2}^2 + C\nu^{-1}(\delta^2 h^{2k} + h^{2k+2})(\sum_{n=1}^{N}\|\ (A^{-1})^n u\ \|_{2,k+1}^2\,) \\
&+C(\Delta t)^4\left(\|u_{ttt}\|_{2,0}^2 + \nu^{-1}\|p_{tt}\|_{2,0}^2 + \|f_{tt}\|_{2,0}^2\right. \\
&\qquad +\nu\|\nabla u_{tt}\|_{2,0}^2 + \nu^{-1}\|\nabla u_{tt}\|_{4,0}^4 \\
&\qquad \left.+\nu^{-1}|||\nabla u|||_{4,0}^4 + \nu^{-1}|||\nabla u_{1/2}|||_{4,0}^4\right)\ .
\end{aligned}
\tag{3.28}
$$

Hence, with $\triangle t$ sufficiently small, i.e. $\triangle t < C(\nu^{-3}|||\nabla u|||_{\infty,0}^4+1)^{-1}$, from Gronwall's Lemma (see (2.14), we have

$$
\begin{aligned}
&\|\phi_M^h\|^2 + \nu\triangle t \sum_{n=0}^{M-1} \|\nabla\phi_{n+1/2}^h\|^2 \\
\leq\ & C\nu^{-1}\,h^{2k+1}\left(|||u|||_{4,k+1}^4 + |||\nabla u|||_{4,0}^4\right) + C\nu h^{2k}|||u|||_{2,k+1}^2 \\
&+C\nu^{-1}h^{2k}\left(|||u|||_{4,k+1}^4 + \nu^{-1}(\|w_0^h\|^2 + \nu^{-1}|||f|||_{2,\star}^2)\right) + C\nu^{-1}h^{2s+2}|||p_{1/2}|||_{2,s+1}^2 \\
&+C\nu^{-1}\delta^{4N+4}\|\overline{u}\|_{2,2N+2}^2 + C\nu^{-1}(\delta^2 h^{2k} + h^{2k+2})(\sum_{n=1}^{N}\|\ (A^{-1})^n u\ \|_{2,k+1}^2\,) \\
&+C(\Delta t)^4\left(\|u_{ttt}\|_{2,0}^2 + \nu^{-1}\|p_{tt}\|_{2,0}^2 + \|f_{tt}\|_{2,0}^2\right. \\
&\qquad +\nu\|\nabla u_{tt}\|_{2,0}^2 + \nu^{-1}\|\nabla u_{tt}\|_{4,0}^4 \\
&\qquad \left.+\nu^{-1}|||\nabla u|||_{4,0}^4 + \nu^{-1}|||\nabla u_{1/2}|||_{4,0}^4\right)\ .
\end{aligned}
\tag{3.29}
$$

Estimate (3.2) then follows from the triangle inequality and (3.29).

To obtain (3.3), we use (3.29) and

$$
\begin{aligned}
&\|\nabla\left(u(t_{n+1/2}) - (w_{n+1}^h + w_n^h)/2\right)\|^2 \\
\leq\ & \|\nabla(u(t_{n+1/2}) - u_{n+1/2})\|^2 + \|\nabla\eta_{n+1/2}\|^2 + \|\nabla\phi_{n+1/2}^h\|^2 \\
\leq\ & \frac{(\triangle t)^3}{48}\int_{t_n}^{t_{n+1}} \|\nabla u_{tt}\|^2\,dt + Ch^{2k}|u_{n+1}|_{k+1}^2 + Ch^{2k}|u_n|_{k+1}^2 + \|\nabla\phi_{n+1/2}^h\|^2\,.
\end{aligned}
$$

□

4 Numerical Experiments

We now present numerical results for the linear extrapolated Algorithm given by

Algorithm 4.1. *[Extrapolated Crank-Nicholson Scheme for Leray-deconvolution] Let* $\Delta t > 0$, $(w_0, q_0) \in (X^h, Q^h)$, $f \in X^*$ *and* $M := \frac{T}{\Delta t}$ *and* $(w_{-1}, q_{-1}) = (w_0, q_0)$. *For* $n = 0, 1, 2, \cdots, M-1$, *find* $(w_{n+1}^h, q_{n+1}^h) \in (X^h, Q^h)$ *satisfying*

$$\frac{1}{\Delta t}(w_{n+1}^h - w_n^h, v^h) + b^*(D_N^h \overline{E(w_n^h, w_{n-1}^h)}^h, w_{n+1/2}^h, v^h) - (q_{n+1/2}^h, \nabla \cdot v^h) + \nu(\nabla w_{n+1/2}^h, \nabla v^h) = (f_{n+1/2}, v^h) \ \forall \ v^h \in X^h \quad (4.1)$$

$$(\nabla \cdot w_{n+1}^h, \chi^h) = 0 \ \forall \chi^h \in Q^h \quad (4.2)$$

where $E(w_n^h, w_{n-1}^h) = \frac{3}{2}w_n^h - \frac{1}{2}w_{n-1}^h$. It is well-known that the choice of the first timestep is critical for computations. For Algorithm 4.1, backward Euler suffices. Then, for $n = 0$, our choice of (w_{-1}, q_{-1}) is just constant extrapolation. The linear extrapolation algorithm for Navier-Stokes equations is investigated in [6] by Baker (and many other subsequently). It is second order in time and requires only the solution of one linear system per time step. The convergence analysis of the extrapolated CN method given by (4.1)-(4.2) follows closely but it is technically longer that the full CN method that we performed in Section 3. The code was written in MATLAB and run on desktop machines. The first computations used Taylor-Hood elements on the periodic box $\Omega = (0, 1)^3$. The averaging radius $\delta = O(h)$ in all performed computations. Because of memory limitation, the 3d computations used meshes only as fine as $h = 1/32$, i.e. 112,724 degrees of freedom. While this is not sufficient for many applications, it is adequate for verifying convergence rates and comparing errors between models. The 3d code utilized MATLAB's conjugate gradient squared method (CGS) to solve the resulting linear systems from both the filtering and the schemes themselves.

4.1 $3d$ Convergence Rate Verification

Our first experiment verifies the predicted error rates proven in Section 3 at $Re = 1$ for the extrapolated trapezoidal Leray-deconvolution schemes $N = 0, 1, 2, 3$. For (P_2, P_1) elements, all four schemes are second order accurate in the H^1 norm. The $N = 0$ scheme is only second order accurate in the L^2 norm, and the other three higher order (in N) schemes are third order accurate in the L^2 norm. *Thus one conclusion is that higher order ($N \geq 1$) Leray-deconvolution models provide better practical accuracy, even after discretization, than the $N = 0$ case of the Leray-alpha model.*

Table 1 contains errors and error ratios for the schemes' approximations to the true solution

$$u = \begin{pmatrix} \cos(2\pi(z+t)) \\ \sin(2\pi(z+t)) \\ \sin(2\pi(x+t)) \end{pmatrix}, \quad p = \sin(2\pi(x+t). \quad (4.3)$$

This particular solution was chosen because it is a simple periodic function with at least a somewhat complex structure: A quick calculation by hand shows that the helicity $H = -2\pi$ for any t, and hence we know there is at least some tangledness and knottedness of vortex lines revealed in Figure 1. For these calculations, we set $\delta = h$ and $\Delta t < h^{3/2}$ (approximately $h^{3/2}$, but a multiple of .005 so that all times line up). Results are given at $t = 0.5$.

4.2 $3d$ Error Comparisons at Re=5000

The goal of the second experiment is to test if the regularizing effect of the Leray-deconvolution model is really advantageous in practical computing. Thus we consider Baker's extrapolated

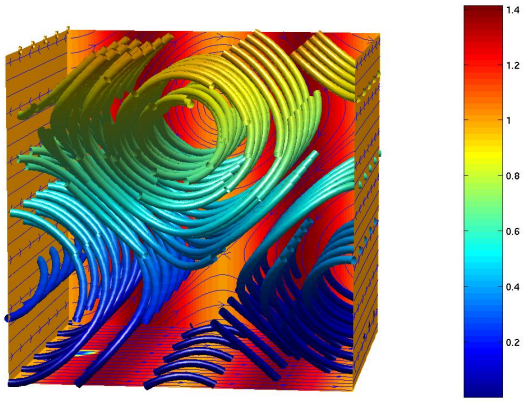

Figure 1: A plot of the initial (t=0) velocity for (4.3)

Table 1: L^2 **and** H^1 **errors and rates at** $Re = 1$ **and t=0.5**

h	$\|u - u^h_{LD0}\|_{L^2}$	ratio	$\|u - u^h_{LD1}\|_{L^2}$	ratio	$\|u - u^h_{LD2}\|_{L^2}$	ratio	$\|u - u^h_{LD3}\|_{L^2}$	ratio
1/8	0.0280	-	0.0245	-	0.0240	-	0.239	-
1/16	0.0061	2.19	0.0032	2.91	0.0032	2.91	0.0032	2.91
1/32	0.0015	2.01	0.0004	2.94	0.0004	2.91	0.0004	2.91
h	$\|u - u^h_{LD0}\|_{H^1}$	ratio	$\|u - u^h_{LD1}\|_{H^1}$	ratio	$\|u - u^h_{LD2}\|_{H^1}$	ratio	$\|u - u^h_{LD3}\|_{H^1}$	ratio
1/8	0.6904	-	0.6789	-	0.6772	-	0.6769	-
1/16	0.1809	1.93	0.1750	1.96	0.1749	1.95	0.1748	1.95
1/32	0.0459	1.98	0.0441	1.99	0.0441	1.99	0.0441	1.99

Crank-Nicolson method (called CNLE) for the NSE and the Leray-deconvolution regularization (called LerayDC) of the NSE.

Figures 2 and 3 present graphs of the L^2 and H^1 errors for the methods vs. time for $Re = 5000$ on our finest mesh $h = 1/32$ and timestep $\Delta t = 0.005$. From these graphs it is clear that *the extrapolated trapezoidal Leray-deconvolution schemes with* $N = 1, 2, 3$ *are all much more accurate than both CNLE and the discrete Leray-alpha model* ($N = 0$ *case)* in the L^2 and H^1 norms. Furthermore, the graphs indicate that *over longer time intervals, the three higher order Leray-deconvolution schemes can remain accurate, whereas the errors in the unregularized CNLE and the lower order regularized Leray-alpha model (LerayDC with* $N = 0$*) can grow catastrophically.*

Figure 2: L^2 Error vs. Time for CNLE and LerayDC with N=0,1,2,3

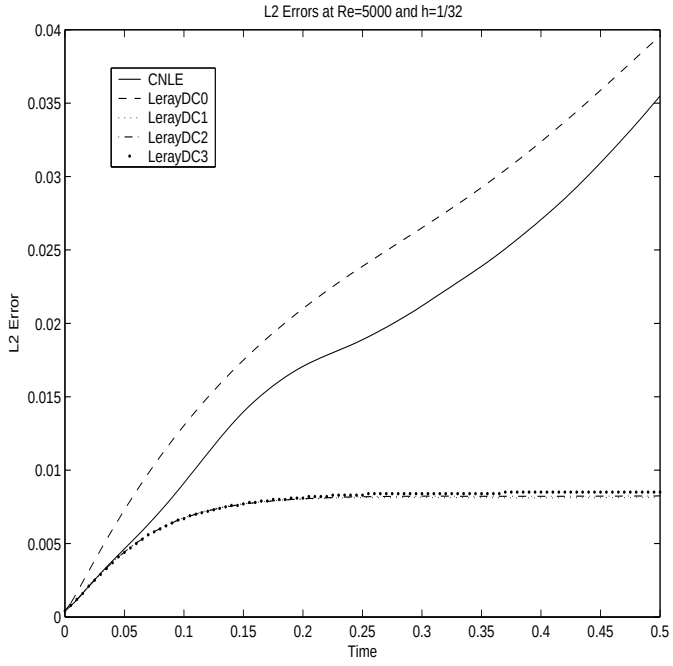

4.3 Underresolved flows in $2d$

Regularization and stabilization can often affect transitional flows negatively. The simplest test of this is to see if the stabilization in the Algorithm 4.1 retards separation of vortices behind a blunt body near the critical Reynolds number for detachment. To do so, we study underresolved flow with recirculation, i.e., the flow across a step. (A discussion of this test problem can be found in Gunzburger [17].) The most distinctive feature of this flow is a recirculating vortex behind the step that detaches in the range $500 \leq Re \leq 700$, see Figure 4 for illustration.

We will study this flow at $\nu = 1/600$ since about this value of ν the flow is in the transition from equilibrium to time dependent, via shedding of eddies behind the step. In our simulations we used Leray Deconvolution Models, i.e. (1.2) with $N = 0$ (LerayDC0), $N = 1$ (LerayDC1) and $N = 2$ (LerayDC2). We will compare these models with one often used for underresolved flow simulation - the Smagorinsky model [8][23][37]. The only difference between the Navier-Stokes equations (NSE) and the Smagorinsky model (SMA) is in the viscous term, which has the following form:

$$\nabla \cdot ((2\nu + 0.01\delta^2 ||\mathbb{D}(u)||_F)\mathbb{D}(u)) .$$

Here, $\mathbb{D}(u)$ is the deformation tensor and $||\cdot||_F$ denotes the Frobenius norm. Although the Smagorinsky model is widely used, it has some drawbacks. These are well documented in the literature, e.g. see [38]: it introduces too much diffusion into the flow, e.g., see Figure 5.

The domain of the two-dimensional flow across a step is presented in Figure 6. We present results for a parabolic inflow profile, which is given by $u = (u_1, u_2)^T$, with $u_1 = y(10 - y)/25$, $u_2 = 0$. No-slip boundary condition is prescribed on the top and bottom boundary as well as on the step. At the outflow we also imposed the parabolic profile or "do nothing" boundary condition.

Figure 3: H^1 Error vs. Time for CNLE and LerayDC with N=0,1,2,3

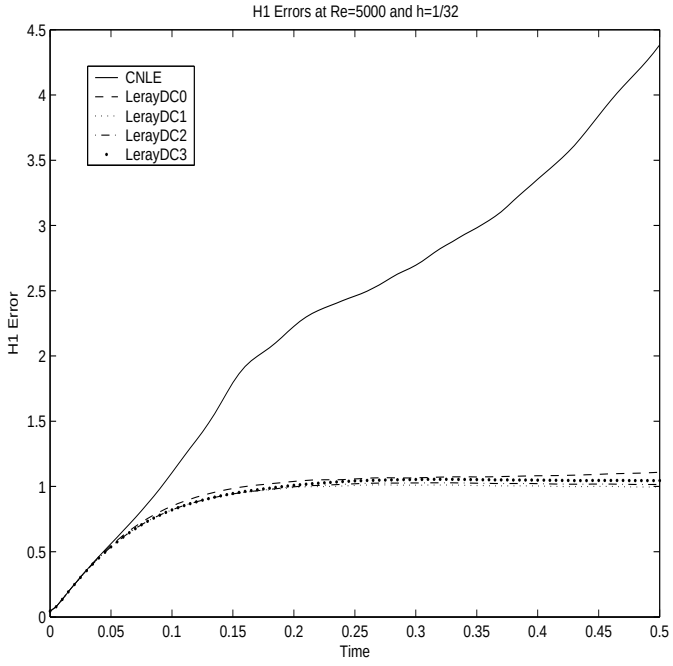

The computations were performed on various grids with the software FreeFem++, [36]. The grid level 3 is the finest with the number of degrees of freedom being 41538. Then the grids level 2, 1 and 0 are coarser with the number of degrees of freedom 27228, 5845 and 1535, respectively. For instance, for the fully resolved NSE simulation, which is our "truth" solution, we used a fine grid (level 3) whereas a much coarser grid (level 1 and level 0) has been used for LerayDC0, LerayDC1, LerayDC2 and SMA. The point is to compare the performance of the various options in underresolved simulations by comparison against a "truth"/fully-resolved solution, Figure 4.

Therefore, the models were discretized in time with the full Crank Nicolson method [3] and in space with the Taylor Hood finite-element.

Comparing the Figures 5, 8, 9, 10 with 4 we conclude that the LerayDC0, LerayDC1

[3]Linear extrapolation was found to induce too much noise that affected the shedding of eddies behind the step. Preliminary tests with quadratic extrapolation were, however, encouraging.

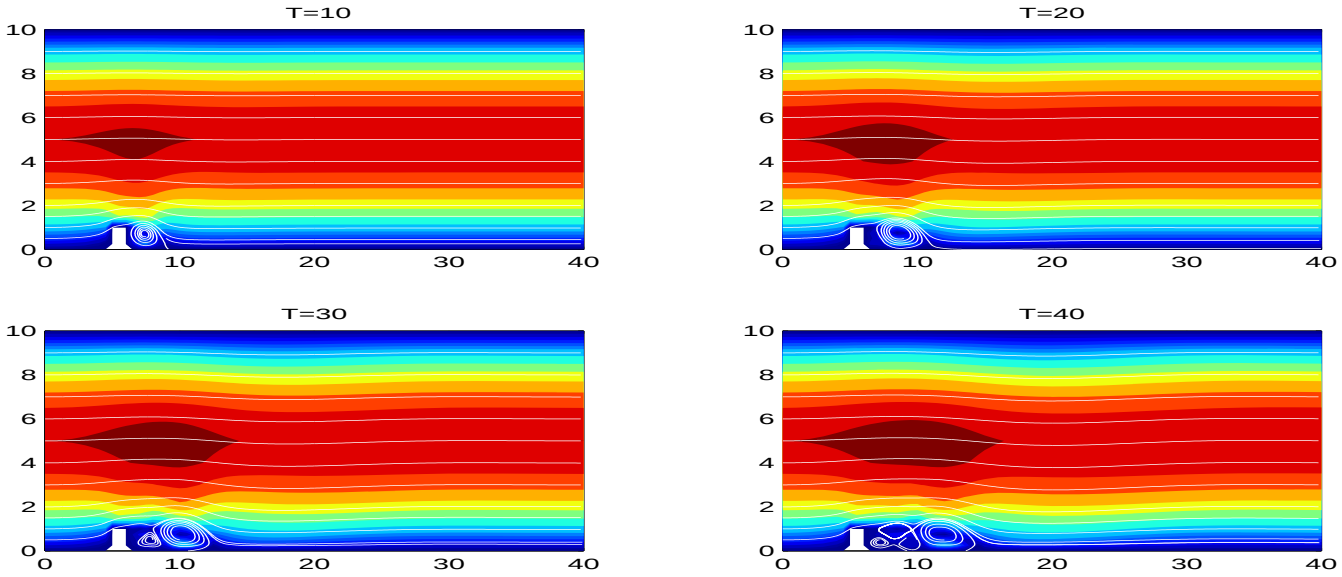

Figure 4: NSE at $\nu = 1/600$, level 3 grid

and LerayDC2 tests replicate the shedding of eddies and the Smagorinsky eddy remains attached. Clearly, the Smagorinsky model is too stabilizing: eddies which should separate and evolve remain attached and attain steady state.

However, regarding the main point of study, *Leray Deconvolution Models improved the simulation results for this transition problem. On the coarsest grid level 0, LerayDC0 failed to shed eddies behind the step but LerayDC1 and LerayDC2 (see Figure 11) still give a successful shedding.*

5 Miscroscale for Leray Deconvolution Models

When the higher order Leray-deconvolution models are used to approximate turbulent flows, an estimate of computational resources required can be obtained by estimating (under the assumptions of isotropy and homogeneity) the model's microscale. This was first performed by Muschinsky [33] for the Smagorinsky model and has been used for other models recently, e.g. [28]. We conclude our study of Leray-deconcvolution models and their discretization by summarizing this analysis.

The Reynolds number for Navier-Stokes equations represents the ratio of nonlinearity over the viscous terms. Then, for the Leray Deconvolution Models (LDMs) we have

$$Re_{model} \simeq \frac{|D_N \overline{\mathbf{u}} \cdot \nabla \mathbf{u}|}{|\nu \triangle \mathbf{u}|}.$$

The model's Reynolds numbers with respect to the model's largest and persistent scales are thus

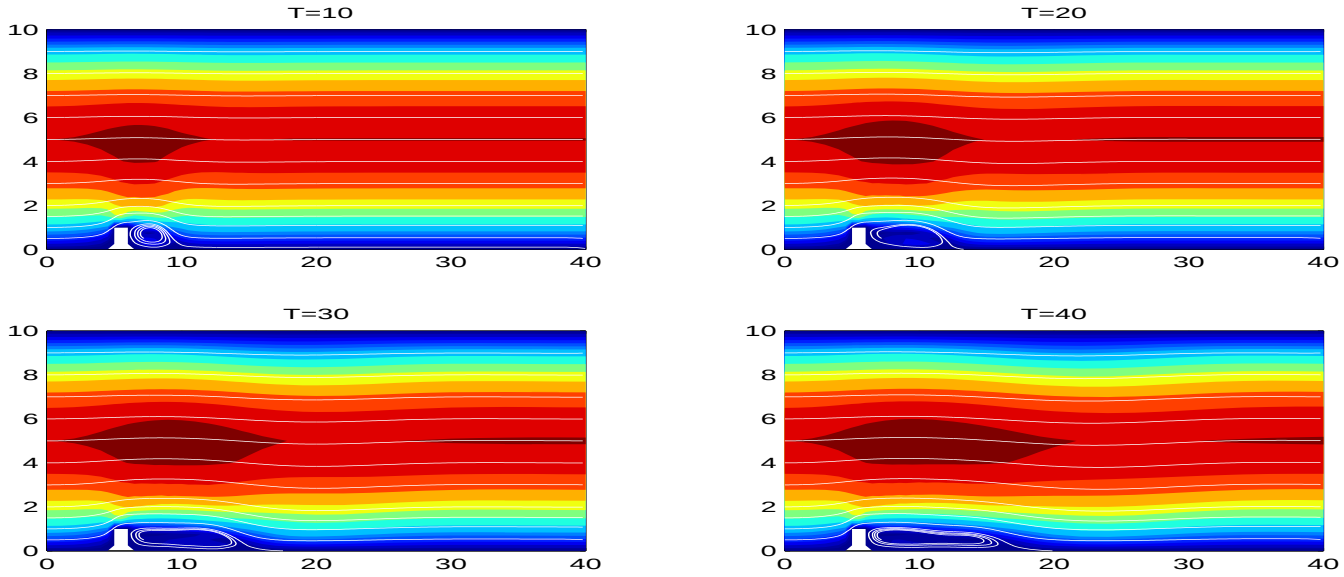

Figure 5: SMA at $\nu = 1/600$, $\delta = 1.5$ and level 1 grid

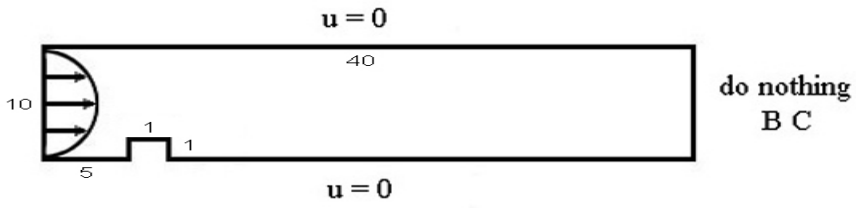

Figure 6: Boundary conditions

$$\text{Large scales:} \qquad Re_{model-large} = \frac{UL}{\nu(1+(\frac{\delta}{L})^2)} \sum_{n=0}^{N} \left(1 - \frac{1}{1+\frac{\delta^2}{L^2}}\right)^n$$

$$\text{Small scales:} \qquad Re_{model-small} = \frac{w_{small}\eta_{model}}{\nu(1+(\frac{\delta}{\eta_{model}})^2)} \sum_{n=0}^{N} \left(1 - \frac{1}{1+\frac{\delta^2}{\eta_{model}^2}}\right)^n .$$

As in the Navier-Stokes equations, any energy cascade in the Leray-deconvolution models is halted by viscosity grinding down eddies exponentially fast when

$$Re_{model-small} = O(1), \text{ i.e., when}$$
$$\frac{w_{small}\eta_{model}}{\nu(1+(\frac{\delta}{\eta_{model}})^2)} \sum_{n=0}^{N} \left(1 - \frac{1}{1+\frac{\delta^2}{\eta_{model}^2}}\right)^n \simeq 1.$$

The characteristic velocity of the model's smallest persistent eddies w_{small} is thus

$$w_{small} \simeq \frac{\nu}{\eta_{model}} \left(\frac{1}{(1+\frac{\delta^2}{\eta_{model}^2})} \sum_{n=0}^{N} \left(1 - \frac{1}{1+\frac{\delta^2}{\eta_{model}^2}}\right)^n \right)^{-1} .$$

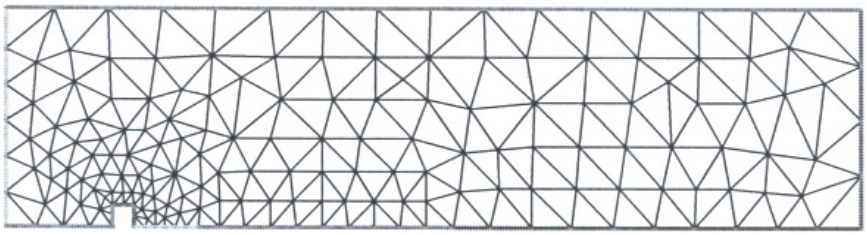

Figure 7: Grid at level 0

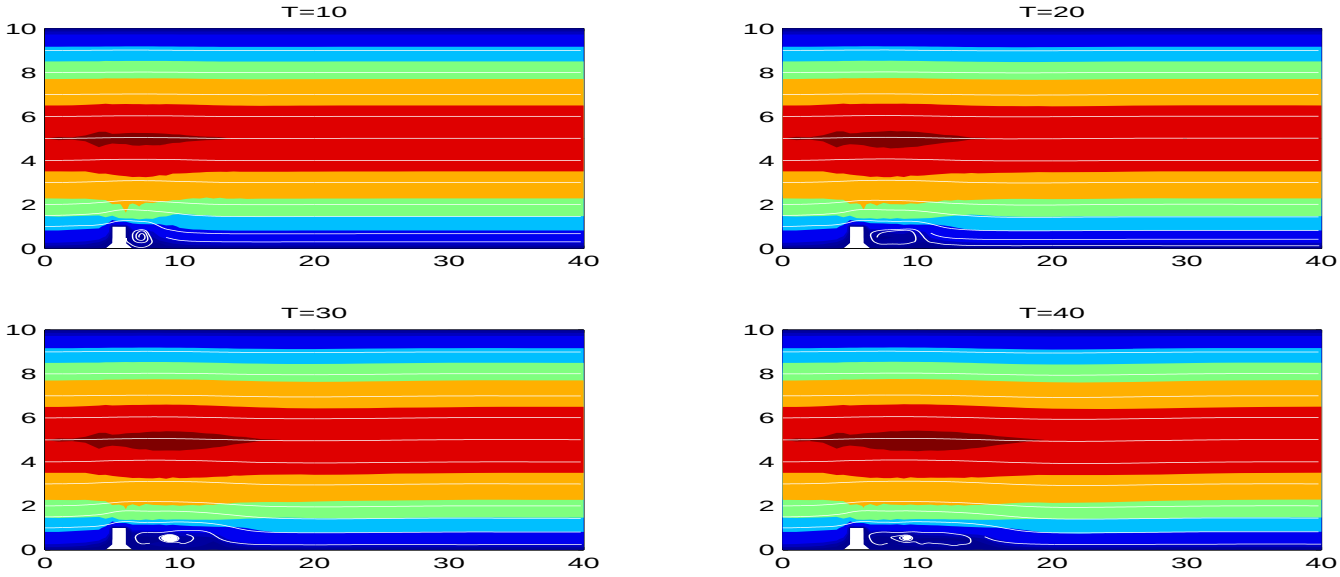

Figure 8: LerayDC0 at $\nu = 1/600$, $\delta = 1.5$ and level 1 grid

The second important equation determining the model's micro-scale comes from statistical equilibrium, i.e., matching energy in to energy out. The rate of energy input to the largest scales is the energy over the associated time scale

$$\frac{E_{model}}{(\frac{L}{U})} = \frac{U^2}{(\frac{L}{U})} = \frac{U^3}{L}.$$

When the model reaches statistical equilibrium, the energy input to the largest scales must match the energy dissipation at the model's micro-scale which scales like $\varepsilon_{small} \simeq \nu(|\nabla w_{small}|^2) \simeq \nu(\frac{w_{small}}{\eta_{model}})^2$. Thus we have

$$\frac{U^3}{L} \simeq \nu(\frac{w_{small}}{\eta_{model}})^2.$$

Inserting the above formula for the micro-eddies characteristic velocity w_{small} gives

$$\frac{U^3}{L} \simeq \frac{\nu^3}{\eta_{model}^4} \left(\frac{1}{(1+\frac{\delta^2}{\eta_{model}^2})} \sum_{n=0}^{N} \left(1 - \frac{1}{1+\frac{\delta^2}{\eta_{model}^2}} \right)^n \right)^{-2} \tag{5.1}$$

Next, the solution to this equation depends on which term in the numerator of the RHS is dominant: 1 or $(\frac{\delta}{\eta_{model}})^2$.

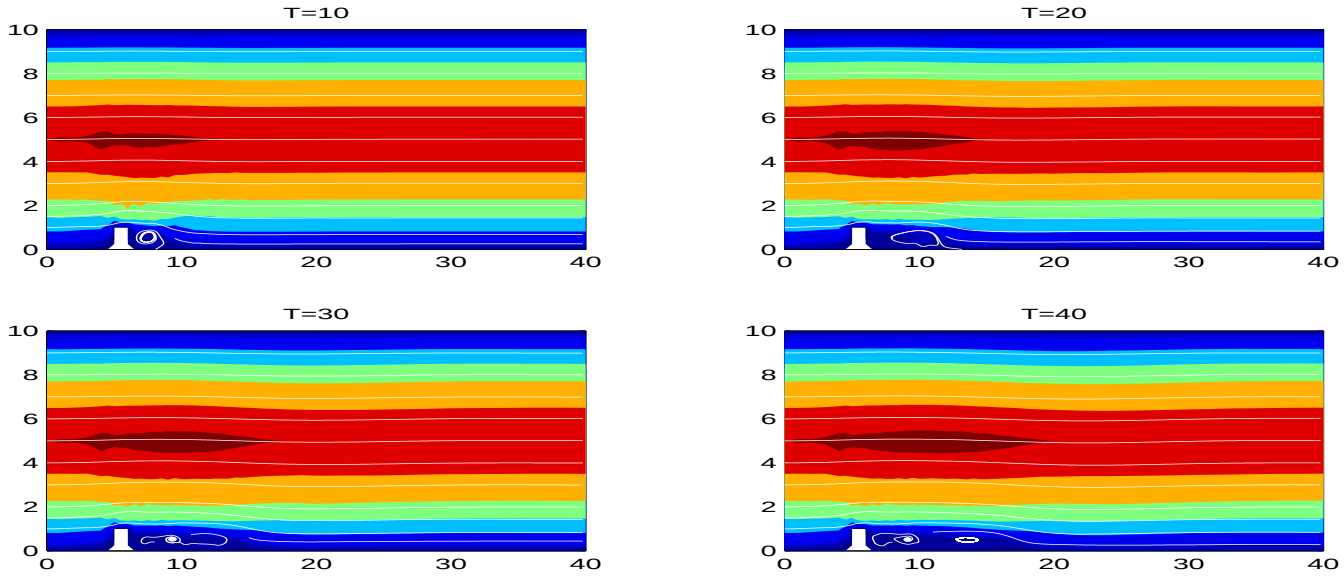

Figure 9: LerayDC1 at $\nu = 1/600$, $\delta = 1.5$ and level 1 grid

Case 1 when $\delta \ll \eta_{model}$, i.e. $1 + \frac{\delta^2}{\eta^2_{model}} \simeq 1$. Then

$$\eta_{model} \simeq Re^{-\frac{3}{4}} L \quad \text{for } N = 0, 1, 2, \ldots.$$

For the case (i) the model predicts the correct microscale, i.e. Kolmogorov microscale since that case occurs when the averaging radius δ is so small that the model is very close to the NSE. However, the latter case is the expected case.

Case 2 when $\delta \gg \eta_{model}$, i.e. $1 + \frac{\delta^2}{\eta^2_{model}} \simeq \frac{\delta^2}{\eta^2_{model}}$. We rewrite equation (5.1).

$$\frac{U^3}{L} \simeq \frac{\nu^3}{\eta^4_{model}} \left(\frac{1}{(1 + \frac{\delta^2}{\eta^2_{model}})} \sum_{n=0}^{N} \left(\frac{\frac{\delta^2}{\eta^2_{model}}}{1 + \frac{\delta^2}{\eta^2_{model}}} \right)^n \right)^{-2}$$

Since $\delta \gg \eta_{model}$ we have

$$\frac{U^3}{L} \simeq \frac{\nu^3}{\eta^4_{model}} \left(\frac{1}{\frac{\delta^2}{\eta^2_{model}}} \sum_{n=0}^{N} \left(\frac{\frac{\delta^2}{\eta^2_{model}}}{\frac{\delta^2}{\eta^2_{model}}} \right)^n \right)^{-2}$$

Therefore,

$$\eta_{model} \simeq Re^{-\frac{3}{4}} L^{1/2} \delta^{1/2} (N+1)^{1/8} \quad \text{for } N = 0, 1, 2, \ldots.$$

The microscale of the Leray Deconvolution models is larger than the Kolmogorov microscale which is $O(Re^{-3/4})$. An interesting result which was observed experimentally too is that the models' microscale is affected by the order of the de-convolution operator, meaning that the increase of N gives more truncation of small scales but preserving high accuracy of the models' solution over the large scales.

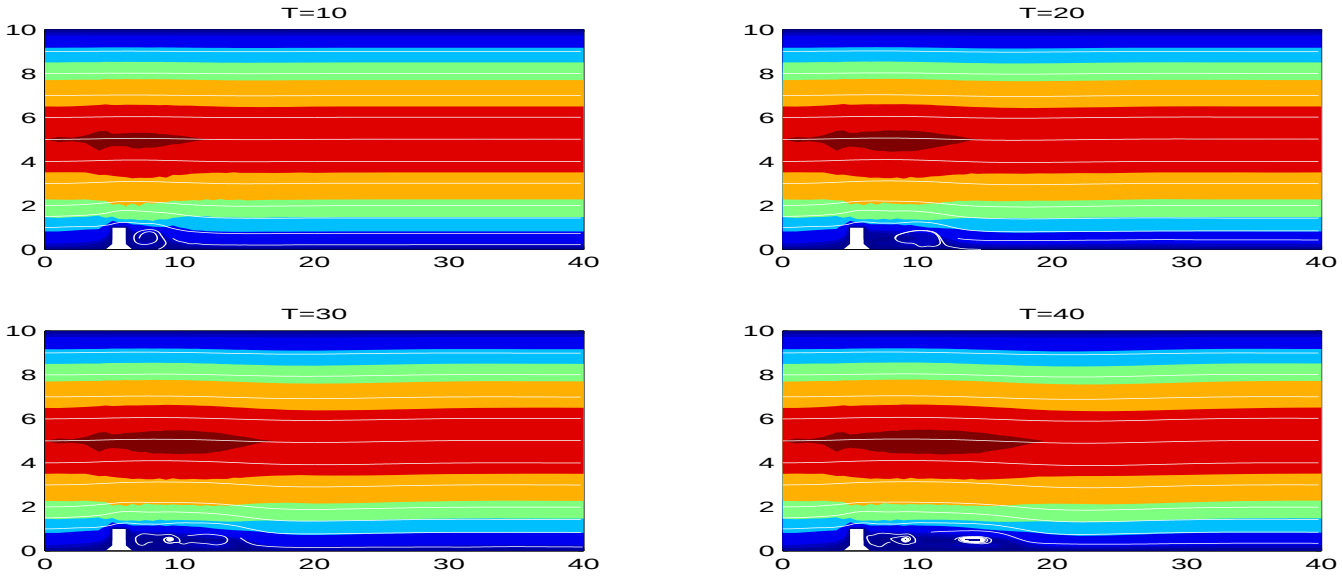

Figure 10: LerayDC2 at $\nu = 1/600$, $\delta = 1.5$ and level 1 grid

6 Conclusions

The van Cittert deconvolution algorithm requires only a few Poisson solves. The condition number of the linear system associated with each solve of $(-\delta^2 \triangle + 1)$ is $O(\delta^2/h^2 + 1)$, i.e. $O(1)$ if $\delta = O(h)$. Thus, the extra complexity of differential filtering and deconvolution is negligable over solving the NSE.

On the other hand, the regularization the higher order Leray-deconvolution models give has remarkable and positive effects on the results of the computations. Errors are observed to be much better over much larger time intervals and the transition from one type of flow to another is not retarded in our experiments as well.

The higher order Leray-deconvolution models had greater accuracy and physical fidelity than the $N = 0$ case (Leray-alpha model).

The experiments we have given were limited by time and resources but their results have consistently showed that: *higher order is to be strongly preferred to lower order*, i.e. LerayDC for higher N to Leray-alpha (the N=0 case).

The form of the Leray-deconvolution model allows an efficient and unconditionally stable timestepping scheme to be used. We have given a convergence analysis which was also verified in $3d$ calculations. Naturally, we believe that further explorations would reveal that higher order extrapolation (e.g. quadratic) would perform even better than the linear extrapolation tested herein.

References

[1] N.A. Adams and S. Stolz, Deconvolution methods for subgrid-scale approximation in large eddy simulation, in *Modern Simulation Strategies for Turbulent Flow*, R.T. Edwards, 2001.

[2] N.A. Adams and S. Stolz, A subgrid-scale deconvolution approach for shock capturing, *J.C.P.*, **178** 391–426, (2002).

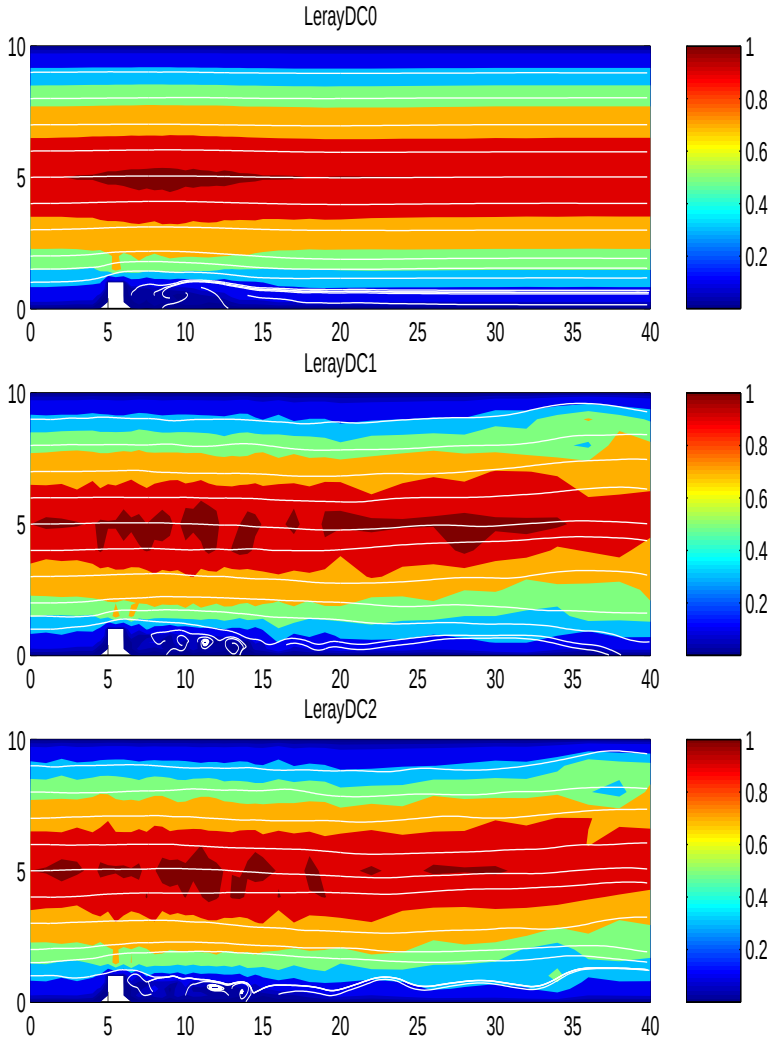

Figure 11: LerayDC0, LerayDC1, LerayDC2, respectively at $T = 40$, $\nu = 1/600$, $\delta = 3.0$ and level 0 grid

[3] N.A. Adams and S. Stolz, An approximate deconvolution procedure for large-eddy simulation, *Phys. Fluids*, **11** 1699–1701, (1999).

[4] N.A. Adams and L. Kleiser and S. Stolz, On the approximate deconvolution model for large-eddy simulations with application to incompressible wall-bounded flows, *Phys. Fluids*, **13** 997–1015, (2001).

[5] N.A. Adams and L. Kleiser and S. Stolz, The approximate deconvolution model for large-eddy simulations of compressible flows and its application to shock-turbulent-boundary-layer interaction, *Phys. Fluids*, **13** 2985–3001, (2001).

[6] G. Baker, Galerkin Approximation for the Navier-Stokes Equations, Report, Harvard University, 1976.

[7] M. Bertero and B. Boccacci, *Introduction to Inverse Problems in Imaging*, IOP Publishing Ltd., 1998.

[8] L.C. Berselli, T. Iliescu and W. Layton, *Mathematics of Large Eddy Simulation of Turbulent Flows*, Springer, Berlin, 2006.

[9] S. Brenner and L.R. Scott, *The Mathematical Theory of Finite Element Methods*, Springer-Verlag, 1994.

[10] V.V.Chepyzhov, E.S. Titi and M.I. Vishik, *On the convergence of the Leray-alpha model to the trajectory attractor of the* $3d$ *Navier-Stokes system*, Report, 2005.

[11] A. Cheskidov, D.D. Holm, E. Olson and E.S. Titi, On a Leray-α model of turbulence, *Royal Society London, Proceedings, Series A, Mathematical, Physical and Engineering Sciences, 461*, 2005, 629-649.

[12] A. Dunca and Y. Epshteyn, On the Stolz-Adams deconvolution LES model, to appear in *SIAM Journal of Math. Anal.*, 2006.

[13] U. Frisch, *Turbulence*, Cambridge University Press, 1995.

[14] G.P. Galdi and W.J. Layton, Approximation of the large eddy in fluid motion II: A model for space-filtered flow, *Math. Models and Methods in the Appl. Sciences*, 10(2000), 343-350.

[15] M. Germano, Differential filters for the large eddy numerical simulation of turbulent flows. *Physics of Fluids*, 29(1986):1755-1757.

[16] M. Germano, Differential filters of elliptic type, *Physics of Fluids*, 29(1986):1757-1758.

[17] M.D. Gunzburger, *Finite Element Methods for Viscous Incompressible Flows - A Guide to Theory, Practices, and Algorithms*, Academic Press, 1989.

[18] J.L. Guermond, S. Prudhomme and J.T. Oden, An interpretation of the NS alpha model as a frame indifferent Leray regularization, *Physica D Nonlinear Phenomena*, 177:23-30, March 2003.

[19] B.J. Geurts and D.D. Holm, Leray and LANS-alpha modeling of turbulent mixing, *J. of Turbulence*, 00(2005), 1-42.

[20] B.J. Geurts and D.D. Holm, Regularization modeling for large eddy simulation, *Physics of Fluids*, 15(2003).

[21] B.J. Guerts, *Elements of direct and large eddy simulation*, Edwards Publishing, 2003.

[22] A.A. Ilyin, E.M. Lunasin and E.S. Titi, *A modified Leray-alpha subgrid-scale model of turbulence*, Report, 2005.

[23] V. John, Large Eddy Simulation of Turbulent Incompressible Flows. *Analytical and Numerical Results for a Class of LES Models*, Lecture Notes in Computational Science and Engineering, vol. 34, Springer-Verlag Berlin, Heidelberg, New York, 2003.

[24] P. Gresho and R. Sani, *Incompressible Flow and the Finite Element Method*, Vol 2., Wiley, 1998.

[25] J.G. Heywood and R. Rannacher, Finite element approximation of the nonstationary Naveri-Stokes problem., Part IV: Error analysis for the second order time discretization, *SIAM J. Numer. Anal.*, 2, 1990, 353-384.

[26] W. Layton, *Introduction to the Numerical Analysis of Incompressible, Viscous Flows*, SIAM to appear, 2007.

[27] W. Layton and R. Lewandowski, On the Leray deconvolution model, Technical Report, University of Pittsburgh, 2005.

[28] W. Layton and M. Neda, Truncation of scales by time relaxation, Technical Report, 2005, to appear in JMAA.

[29] J. Leray, Essay sur les mouvements plans d'une liquide visqueux que limitent des parois, *J. math. pur. appl.*, Paris Ser. IX, 13(1934), 331-418.

[30] J. Leray, Sur les mouvements d'une liquide visqueux emplissant l'espace, *Acta Math.*, 63(1934), 193-248.

[31] J. Liu and W. Wang, Energy and helicity preserving schemes for hydro and magnetohydro-dynamic flows with symmetry, *Journal of Computational Physics* 2004, 200:8-33.

[32] C. Manica and S. Kaya Merdan, Convergence analysis of the finite element method for a fundamental model in turbulence, Technical Report, University of Pittsburgh, 2006 (submitted).

[33] A. Muschinsky, A similarity theory of locally homogeneous and isotropic turbulence generated by a Smagorinsky-type LES, *JFM*, 325(1996), 239-260.

[34] L. Rebholz, Conservation Laws of turbulence models, to appear in *Journal of Mathematical Analysis and Applications*, 2006.

[35] L. Rebholz, An energy and helicity conserving finite element scheme for the Navier-Stokes equations, In review.

[36] F. Hecht and O. Pironneau, FreeFem++ webpage: http://www.freefem.org.

[37] P. Saugat, *Large eddy simulation for incompressible flows*, Springer-Verlag, Berlin, 2001.

[38] R.L. Street Y. Zang and J.R. Koseff, A dynamics mixed subgrid-scale model and its application to turbulent recirculating flows, *Phys. Fluids A* (1993), no. 5, 3186–3196.

[39] M.I. Vishik, E.S. Titi and V.V. Chepyzhov, Trajectory attractor approximations of the 3d Navier-Stokes system by the Leray-alpha model, *Russian Math Dokladi*, 71(2005), 91-95.

[40] E. Zeidler, *Applied Functional Analysis: Applications to Mathematical Physics*, Springer-Verlag, New York, 1995.